Journal of Power Sources 195 (2010) 3323–3327

Contents lists available at ScienceDirect

Journal of Power Sources

journal homepage: www.elsevier.com/locate/jpowsour

Short communication

Lithium silicon sulfide as an anode material in all-solid-state lithium batteries

Bui Thi Hang, Tsuyoshi Ohnishi, Minoru Osada, Xiaoxiong Xu, Kazunori Takada*, Takayoshi Sasaki

International Center for Materials Nanoarchitectonics, National Institute for Materials Science, Namiki 1-1, Tsukuba, Ibaraki 305-0044, Japan

ARTICLE INFO

Article history:
Received 28 September 2009
Received in revised form
27 November 2009
Accepted 27 November 2009
Available online 5 December 2009

Keywords:
Anode material
Lithium silicon sulfide
Iron sulfide
Solid-state lithium battery
Pulsed laser deposition

ABSTRACT

The electrochemical properties of Li_2SiS_3 were investigated in a solid electrolyte. Li_2SiS_3 was converted to elemental Si, and the resultant Si was formed into Si–Li alloy in the reduction process; however, the reverse reaction was not completed due to the loss of electronic conduction upon reoxidation. FeS was dispersed as a conductive additive in Li_2SiS_3 films by pulsed laser deposition (PLD). The addition allowed successive reactions to proceed at a large capacity with small capacity-fading during the cycling process in spite of the small FeS fraction. This result indicates that Li_2SiS_3 + FeS thin film is a promising anode for solid-state lithium batteries.

1. Introduction

Today's increasing demand for high-energy batteries requires novel anodes and cathodes that can store more charge. Graphite is commonly used as the anode material in commercial lithium-ion batteries; however, its theoretical capacity is limited (372 mAh g^{-1}, LiC_6). Numerous alternatives to this material have been investigated, one of which is the "conversion electrode" proposed by Poizot et al. [1]. They observed high capacity of about 700 mAh g^{-1} in the reversible conversion reaction from transition metal oxides (MO, where M is Co, Ni, Cu or Fe) to their corresponding elemental transition metals, expressed by:

$$MO + 2Li \leftrightarrow Li_2O + M$$

When an element is formed into an alloy with lithium for use as M, the alloying reaction should give additional capacity. Although such successive reactions seem promising for realizing a high-capacity anode, previous studies have reported that only one reaction proceeds; for example, only the alloying reaction for tin oxides [2] and only the conversion reaction for zinc phosphides [3].

In this study, the electrode properties of Li_2SiS_3 were investigated because Si is expected to show a four-electron reaction in the conversion process and form high Li-content alloys in the following process to give high capacity. When the conversion reaction in Eq. (1) and the alloying reaction in Eq. (2) proceed in succession, the theoretical capacity reaches 8014 mAh g^{-1} for Si (8.4 e/Si), which is much larger than that of graphite or Si (4200 mAh g^{-1} corresponding to the formation of $Li_{4.4}Si$ alloy).

$$Li_2SiS_3 + 4Li^+ + 4e \leftrightarrow 2Li_2S + Si \quad (1)$$

$$Si + 4.4Li^+ + 4.4e \leftrightarrow Li_{4.4}Si \quad (2)$$

In this study, a solid electrolyte was used to investigate electrode properties. The morphology of the electrode greatly affects the electrode properties based on conversion or alloying reactions; for example, change in particle size or degree of aggregation often results in rapid capacity-fading. In contrast, such morphological changes may be suppressed in solid electrolytes because only lithium ions are mobile in the electrolyte; there is no other transport to cause division or aggregation of the active materials. Especially, many studies on Si have shown that the reduction of particle size improves the cycle performance of Si [4,5]. Since single-ion conduction inhibits particle growth in solid electrolytes, Si particles resulting from the conversion reaction would be very small. In fact, the particle size of Fe formed by electrochemical reduction of Li_2FeS_2 in a solid electrolyte is in the order of nanometers or less [6]. These are significant advantages of solid electrolytes for realizing successive reaction.

* Corresponding author. Tel.: +81 29 860 4317; fax: +81 29 854 9061.
E-mail address: takada.kazunori@nims.go.jp (K. Takada).

0378-7753/$ – see front matter © 2009 Elsevier B.V. All rights reserved.
doi:10.1016/j.jpowsour.2009.11.136

2. Experimental

2.1. Sample preparation

Li_2SiS_3 was prepared by mechanical milling using a Fritsch Pulverisette high-energy planetary ball mill. Li_2S (Idemitsu Kansan, 99% purity) and SiS_2 (Furukawa, 99% purity), used as starting materials, were mixed at 1:1 molar ratio and then milled in a sealed agate pot at a rotation speed of 400 rpm for 24 h. In order to investigate the effect of electronic conduction on the electrochemical behavior of Li_2SiS_3, 10 wt% of FeS was added before milling. Si (Kanto Chemical, 99.99% purity) also milled in 96 h to make fine powder was used as a comparison. The electrode properties of the samples were investigated in both powder and thin-film form.

Thin-film samples were prepared by PLD. The powders obtained above were pressed into pellets, which were used as the targets. They were ablated by a KrF excimer laser ($\lambda = 248$ nm) operated at 10 Hz. The laser beam was directed at the target at an incident angle of 60° from the normal and at laser energy of 10 mJ. Thin films were deposited on stainless steel substrates (1 cm in diameter) kept at room temperature. The weight of the film was measured by an electric balance and used to estimate the thickness.

2.2. Measurement

The prepared samples were characterized by powder X-ray diffraction (XRD), Raman spectroscopy, and scanning electron microscope (SEM) observation. The powder XRD data were taken for the samples sealed in a sample holder with an Al window on a diffractometer with Cu Kα radiation (RINT 2200-PC, Rigaku). For the Raman spectroscopy, the samples were also put into an airtight sample holder with a thin glass window. Raman spectra were measured with the 514.5 nm line from an Ar^+ laser by focusing on a 1–2 μm in diameter spot on the sample surface. The backward scattering light was collected and dispersed by a subtractive triple spectrometer HORIBA-Jobin-Yvon T 64000 equipped with a charge couple device detector. SEM images of the samples were taken on KEYENCE VE-8800 microscope.

Electrode properties of the samples were investigated in two-electrode solid-state cells. Glass ceramic with the composition $70Li_2S–30P_2S_5$ [7] was used as the solid electrolyte. The powdered electrolyte was placed in a hole (diameter 10 mm) of an insulator tube and pressed into a pellet. The thin film of Li_2SiS_3 or Li_2SiS_3 + 10 wt% FeS was pressed onto one side of the electrolyte pellet as the working electrode. On the other hand, when the electrode properties of the powder samples were investigated, the samples were mixed with the electrolyte (1:1 weight ratio) and pressed between the electrolyte layer and a stainless steel plate used as a current collector. The counter electrode was In–Li alloy pressed onto the other side of the electrolyte pellet.

The electrochemical cells were cycled at a constant current of 0.01C within a voltage range of −0.62 to 2 V for the powder samples and −0.615 to 2 V for the thin-film samples. The cycling test was performed at room temperature using a multi-channel potentiogalvanostat (PS-08, Toho-Giken).

It should be noted that voltages in this paper including the figures are expressed by adding 0.62 V to the cell voltages. Although In–Li alloy is used as the counter electrode, data for electrochemical cells with Li counter electrodes are much more familiar. Therefore, the potential of In–Li alloy (0.62 V) is added to show the data as if lithium metal were used as the counter electrode.

3. Results and discussion

First of all before going to the electrochemical properties of the samples, their characterization results are shown here. Fig. 1 shows the XRD patterns of the powder samples, i.e. Li_2SiS_3 and that mixed with FeS. Sharp reflections observed in the starting materials (not shown) disappear upon the milling, suggesting the amorphous nature of the materials. However, weak reflections still survived in the pattern for the Li_2SiS_3 mixed with FeS, most of which were assignable to the reflection from FeS. One at $2\theta = 26°$ may be 1 0 0 reflection of Li_2FeS_2, which is a conceivable product by the ball milling.

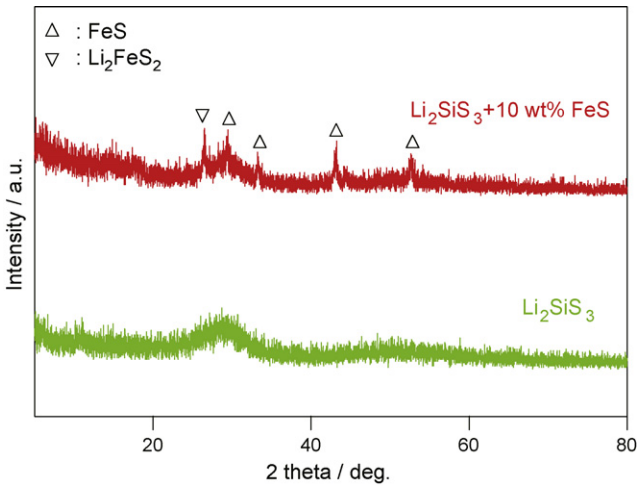

Fig. 1. Powder XRD diffraction patterns of Li_2SiS_3 powder and that mixed with FeS.

On the other hand, characterization of the thin films by XRD is difficult because of the thinness and the hygroscopicity; therefore, they were characterized by Raman spectroscopy. Every sample gave a broad band in a range of 360–400 cm^{-1} in the Raman spectrum as shown in Fig. 2. Such a broad band is characteristic of amorphousness; moreover, the spectra taken from the thin films were very similar to that from the Li_2SiS_3 powder, and thus it can be concluded that the powder sample of Li_2SiSi_3 prepared by ball milling and thin films prepared by PLD are amorphous.

Si was crystalline even after the ball milling of 96 h, which was confirmed by XRD. The ball milling reduced the particle size to less than one micrometer and formed some aggregated domains of several micrometers as shown in the SEM images in Fig. 3.

The charge–discharge profile of the Li_2SiS_3 powder is shown in Fig. 4a. A plateau with a large capacity of 2500 mAh g^{-1} appears in the first reduction process below 0.5 V; such a large capacity is

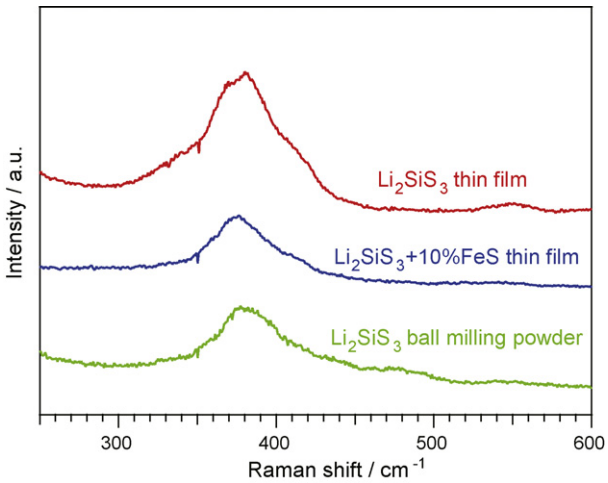

Fig. 2. Raman spectra of Li_2SiS_3 powder and thin film and Li_2SiS_3 + FeS thin film.

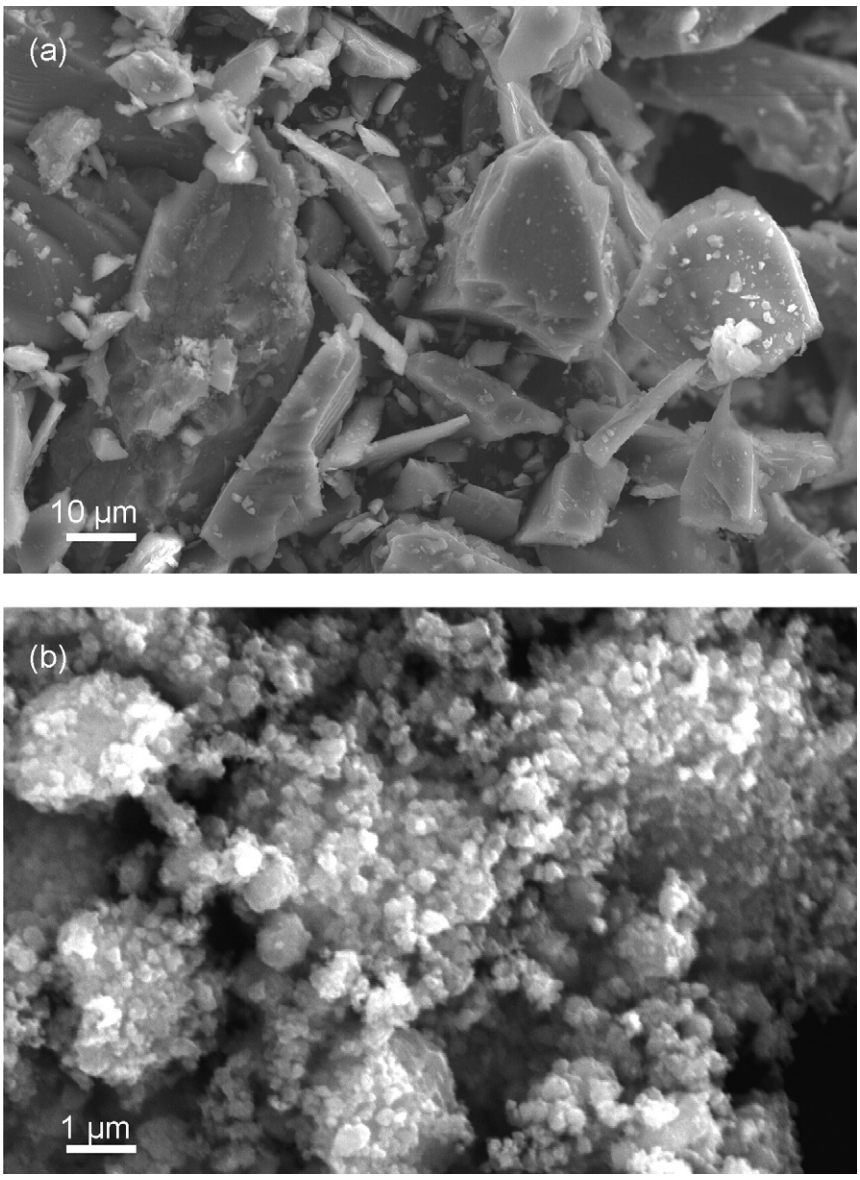

Fig. 3. SEM images of Si powder (a) before and (b) after 96 h ball milling.

explainable only by successive reactions, i.e., reduction of Li_2SiS_3 to elemental Si and the proceeding formation of Si–Li alloy.

It should be noted that the observed capacity exceeds the theoretical value (1630 mAh g^{-1}) corresponding to the reduction of Li_2SiS_3 into Si–$Li_{4.4}$ via elemental Si. In solid electrolytes, crystal growth is suppressed due to the immobility of any species other than lithium ions. For example, Fe particles resulting from the reduction of Li_2FeS_2 in a solid electrolyte are in the order of nanometers in size. Si particles resulting from the reduction in the present study would also be very small, which may give the excess capacity due to the large surface area; even though the lithium composition in bulk is limited to Si–$Li_{4.4}$, the surface may be an exception. In spite of the large capacity observed in the first reduction, only a small capacity was observed in the reoxidation process. It is necessary to increase the coulombic efficiency in the first cycle in order to utilize the material as a high-capacity anode in solid-state batteries.

When the cycling starts with Si in place of Li_2SiS_3 as a comparison, the efficiency is not so low as shown in Fig. 4b. Therefore, it can be concluded that the alloying and dealloying reactions are reversible, and the reason for the low efficiency is in the oxidation process from Si to Li_2SiS_3 or other sulfides. Since the sulfides are electronically insulating, they would interrupt the electronic conduction to terminate the reoxidation, even though Si–Li_x alloys still remain. In other words, the insulating Li_2SiS_3 is converted to semiconducting Si and then to metallic Si–Li alloy in the reduction process, which enhances electronic conduction to promote the electrode reaction. On the contrary, the electrode becomes insulating upon reoxidation, which depresses the electrode reaction and lowers the coulombic efficiency.

The usual way to overcome this problem is to incorporate conductive additives and reduce particle size to prevent the rate being limited by poor electronic conduction. In order to know how small the particles should be, or how short the transport length of electrons should be so as not to limit the reaction rate, Li_2SiS_3 was formed into thin films with different thicknesses by PLD. At a thickness of 1 μm (Fig. 5a), the charge–discharge curves were very similar to those for the powder sample (Fig. 4a). Indeed, decreasing thickness increased the coulombic efficiency, as shown in Fig. 5b; however, it was still only 50% even at a thickness of 100 nm. The

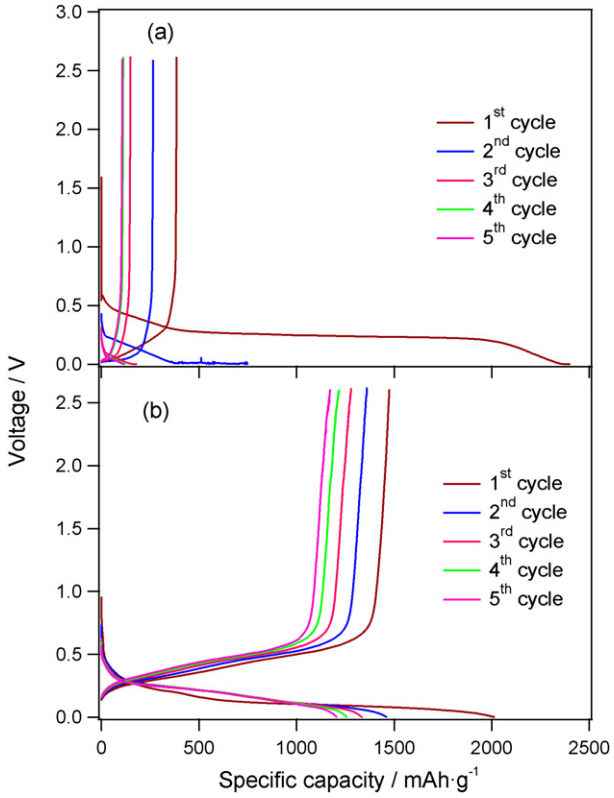

Fig. 4. Charge–discharge profile of (a) Li_2SiS_3 powder and (b) Si powder.

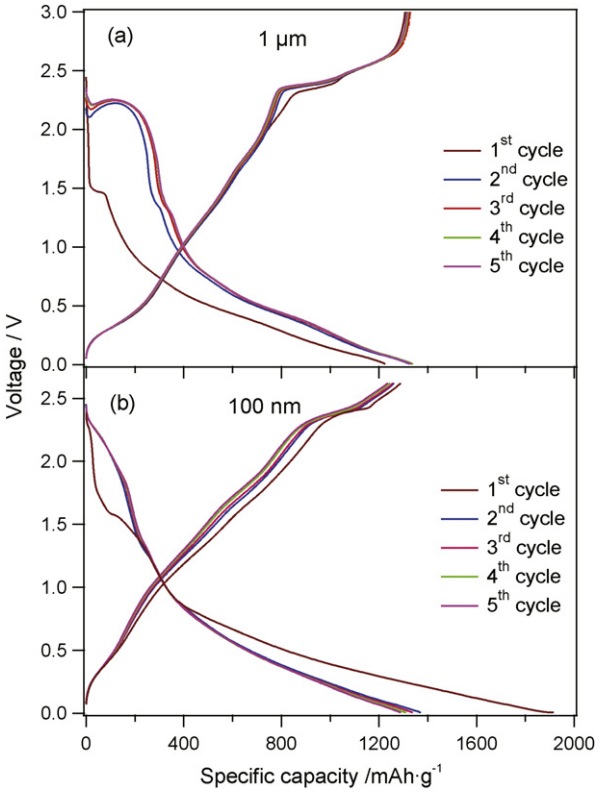

Fig. 6. Charge–discharge profile of Li_2SiS_3 + 10 wt% FeS thin films with different thicknesses.

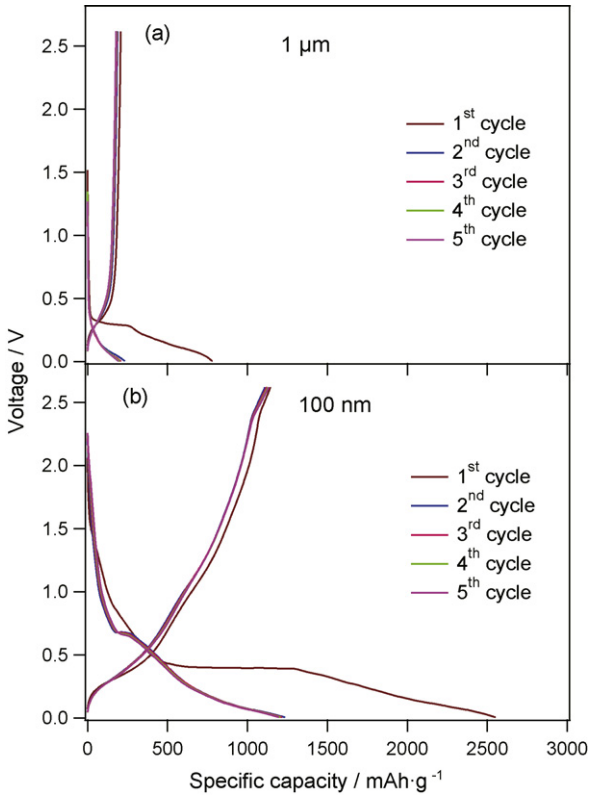

Fig. 5. Charge–discharge profile of Li_2SiS_3 thin films with different thicknesses.

results suggest that the particle size of Li_2SiS_3 should be tens of nanometers for high coulombic efficiency. In fact, although the results are not shown, incorporation of a conductive additive alone does not improve the coulombic efficiency. When Li_2SiS_3 was mixed with FeS as the conductive additive in powder form, the efficiency was still very low.

However, such nanoparticles are not suitable for practical use. Since the nanoparticles have to be loaded on the surface of the conductive additives, the volumetric and gravimetric fraction of conductive additives in such electrodes would be very high, which would lower the energy density of the battery. A practical way to increase the efficiency would be to reduce the particle size of the conductive additives as well and distribute them uniformly among the Li_2SiS_3 particles. Such electrode materials can be prepared by PLD. When a target is ablated by a pulse laser, the material is decomposed once into atomic scale and integrated into the deposited film. This means that Li_2SiS_3 and the conductive additives would be mixed at the atomic level in the film, when their mixture is used as the target.

Fig. 6 shows the electrode properties of thin films deposited from the target of a mixture of Li_2SiS_3 and FeS. When the FeS was introduced in the film as a conductive additive, the electrode performance was greatly improved. Even though the film was 1 μm in thickness (Fig. 6a), the efficiency was almost 100% and the observed capacity was about 1300 mAh g^{-1}, which is comparable to the theoretical value corresponding to 8.4 e.

The charge–discharge curves consisted of several potential steps. Conceivable reactions in the electrode are not only the conversion reaction of Li_2SiS_3 and the alloying reaction of Si but also the redox reaction between Fe and FeS; although FeS was added as an electronic conductor, it shows a redox reaction at 1.6 V in solid-state cells [8]. In fact, a short plateau appeared at 1.6 V in the charge–discharge curves, which suggests that FeS acted not only as a conductive additive but also as an active material in the electrode.

Other plateaus between 2 and 2.5 V and below 1 V are attributable to the conversion and alloying reactions, respectively. By taking into account that Li_2FeS_2 shows a redox reaction at 2.3 V and a trace amount of Li_2FeS_2 was detected in the target by XRD, the former may also come from the redox reaction of Li_2FeS_2 or other Li–Fe–Si–S compounds formed during PLD deposition. However, the amount of FeS is too small to give the capacity observed in the potential plateau, and thus it can be concluded that the potential plateau between 2 and 2.5 V is mainly originated from the conversion reaction. That is to say, all the conceivable reactions appeared as potential plateaus in the charge discharge curves. These results indicate that PLD preparation effectively introduced electronic conduction paths to completely utilize the active material without increasing the fraction of conductive additives.

In addition, the film demonstrated good cycle performance. Although the reaction products must be kept in nanoparticles for the reactions to proceed, the capacity-fading upon cycling was very small. This suggests that the solid electrolyte effectively inhibits mass transfer other than lithium ions to adequately stabilize the nanostructure.

Finally, we summarize the advantages of the electrode prepared by PLD. The most important feature is that PLD preparation effectively provides electronic conduction to the electrode without decreasing the fraction of the active material. The second point is that the preparation method is not only for thin-film electrodes. Although the electrode is a thin film, its thickness is about 1 μm, which is comparable to the particle size of active materials usually used in commercialized cells. Since laser ablation can also be used for powder synthesis [9], such a nanostructure, or homogeneous distribution of active materials and conductive additive at the atomic scale, would also be realized in powder materials for composite electrodes.

4. Conclusions

Considering that the conversion and alloying processes are high-capacity anode reactions in lithium batteries, a material that shows them as successive reactions would be an anode that realizes a battery with high-energy density. Li_2SiS_3 as one of the candidates is actually converted to elemental Si and formed into a Li–Si alloy successively upon reduction. However, little of the resultant alloy returns to the sulfide due to its insulating nature interrupting the reoxidation process. FeS is added as a conductive additive to the Li_2SiS_3 and formed into a film by PLD. Since the PLD disperses atomic-level FeS electronic conduction paths in the film, the electrode performance is drastically improved. The film shows excellent cycling performance and large capacity, indicating that it is a promising candidate for negative electrode material in solid-state lithium batteries.

Acknowledgements

The glass–ceramic solid electrolyte was kindly provided by Idemitsu Kosan Co., Ltd. This study was partly supported by the Li-EAD project of the New Energy and Industrial Technology Development Organization (NEDO).

References

[1] P. Poizot, S. Laruelle, S. Grugeon, L. Dupont, J.M. Tarascon, Nature 407 (2000) 496.
[2] Y. Idota, T. Kubota, A. Matsufuji, Y. Maekawa, T. Miyasaka, Science 276 (1997) 1395.
[3] C.M. Park, H.J. Sohn, Chem. Mater. 20 (2008) 6319.
[4] H. Li, X. Huang, L. Chen, G. Zhou, Z. Zhang, D. Yu, Y.J. Mo, N. Pei, Solid State Ionics 135 (2000) 181.
[5] C.K. Chana, R. Ruffob, S.S. Hong, R.A. Huggins, Y. Cui, J. Power Sources 189 (2009) 34.
[6] K. Takada, Y. Kitami, T. Inada, A. Kajiyama, M. Kouguchi, S. Kondo, M. Watanabe, M. Tabuchi, J. Electrochem. Soc. 148 (2001) A1085.
[7] F. Mizuno, A. Hayashi, K. Tadanaga, M. Tatsumisago, Adv. Mater. 17 (2005) 918.
[8] B.-C. Kim, K. Takada, N. Ohta, Y. Seino, L. Zhang, H. Wada, T. Sasaki, Solid State Ionics 176 (2005) 2383.
[9] A. Gurav, T. Kodas, T. Pluym, Y. Xiong, Aerosol Sci. Technol. 19 (1993) 411.